Nitrogen-Atom Transfer from [PW 11 O 39 Ru VI N] 4– to PPh 3

Claire Besson, Yurii Geletii, Françoise Villain, Richard Villanneau, Craig Hill, Anna Proust

Nitrogen-Atom Transfer from $[PW_{11}O_{39}Ru^{VI}N]^{4-}$ to PPh_3

Claire Besson,[a,b] Yurii V. Geletii,[b] Françoise Villain,[a,c] Richard Villanneau,[a] Craig L. Hill,[b] Anna Proust[a]*

a. *Institut parisien de chimie moléculaire, UMR 7071, Case courier 42, Université Pierre et Marie Curie (Paris 6), 4 place Jussieu, 75252 Paris cedex, France.* anna.proust@upmc.fr.
b. *Department of chemistry, Emory University, Atlanta GA 30322, USA.*
c. *Synchrotron SOLEIL, l'Orme des Merisiers, Saint-Aubin BP 48, 91192 Gif sur Yvette, France.*

Abstract

The nitrido derivative $(n\text{-}Bu_4N)_4[PW_{11}O_{39}Ru^{VI}N]$ transfers its nitrogen atom to triphenylphosphine to give quantitatively the bis(triphenylphosphane)iminium cation $[Ph_3PNPPh_3]^+$. A intermediate can be prepared by the reaction of a single molecule of triphenylphosphine with the polyoxometalate, the iminophosphorate derivative $(n\text{-}Bu_4N)_3[PW_{11}O_{39}Ru^{V}\{NPPh_3\}]$. The reactivity of the latter species has been investigated to complete the general scheme of the nitrogen transfer reaction. By addition of one equivalent of hydroxide, $[PW_{11}O_{39}Ru^{III}\{N(OH)PPh_3\}]^{4-}$ is obtained. The reaction can be reversed by the addition of one proton. The phosphinoxime derivative $[PW_{11}O_{39}Ru^{III}\{N(OH)PPh_3\}]^{4-}$ can be prepared in solution, but is unstable. It decomposes to yield quantitatively $(n\text{-}Bu_4N)_4[PW_{11}O_{39}Ru^{III}\{OPPh_3\}]$. All those species have been thoroughly characterized by mass spectrometry, paramagnetic ^{31}P NMR, IR, Raman, UV-visible, XANES and EXAFS spectroscopies.

Introduction

The chemistry of ruthenium encompasses a wide range of reactions,[1] such as olefin metathesis,[2] solar energy conversion,[3] atom transfer,[4,5] to cite only a few examples. In the latter case, as in most oxidation catalysts, one of the significant problems encountered is the degradation of the ligand and subsequent loss of activity of the catalyst.

Lacunary polyoxometalates, *i. e.* polyoxometalates (POMs) formally lacking metallic centers, are a class of all-inorganic ligands with a set of properties, *e. g.* multidenticity, rigidity, hydrolytical (providing pH control) thermal and oxidative stability, which makes them quite attractive for oxidation catalysis.[6-8] In particular, the past decade has witnessed the growing interest for the incorporation of noble-metal cations into POMs[9] and has underlined the unique ability of POMs to stabilize transition metal cations with high oxidation states.[10-13] A similar quest for high oxidation state ruthenium containing POMs[14,15] has very recently come to a head with the report of an adamantane-like Ru(IV) tetramer stabilized by two divacant decatungstosilicates[16] which proved to be catalytically active towards water oxidation.[17-19] Stabilization of high oxidation states should be easier with the more π electron-donating nitrido ligands and indeed $[PW_{11}O_{39}\{RuN\}]^{4-}$ (**1**) formally includes a Ru(VI) center, from which we evidenced the first nitrogen atom transfer from a functionalized POM.[20] We present here a more detailed analysis of the reactivity of the iminophosphorane $[PW_{11}O_{39}Ru^{V}\{NPPh_3\}]^{3-}$ (**2**). Very little is known about the reactivity of iminophosphorane complexes in general,[21,22] and almost nothing in the case of ruthenium.[23] Our contribution also provides spectroscopic characterization of ruthenium in various oxidation states in the POM, which might be useful to elucidate the reaction mechanisms of ruthenium-containing POMs. This will complete the analytical data gathered in the seminal article by Pope et al. in 1992[24] and more recent papers from Sadakane et al.[25-27]

Experimental section

Instrumentation and techniques of measurement. IR spectra were recorded from KBr pellets (dilution approximatively 2% in weight) on a Bio-Rad Win-IR FTS 165 FT-IR spectrophotometer. Raman spectra were recorded on a Kaiser Optica Systems HL5R spectrometer equipped with a near-IR laser diode working at 785 nm. The laser power was set to 8 mW. Solid samples were used for all compounds, except for $(n\text{-}Bu_4N)_4[PW_{11}O_{39}Ru^{III}\{N(OH)PPh_3\}]$ (**3**). In the latter case, a 4.4 mM solution in acetonitrile was used. UV-visible spectra were acquired on an Agilent 8453 UV-vis spectroscopy system or on a Shimadzu UV-2101 spectrophotometer and, for fast kinetics, on a High-Tech SF-61SX2 stopped flow system equipped with a Bentham M300 monochromator.

Kinetic data analysis was performed using Gepasi software [28] for numerical integration and fit. The ^{31}P (121.5 MHz), ^{13}C (75.6 MHz) and ^{1}H (300 MHz) NMR spectra were obtained at 300 K in 5 mm o. d. tubes on a Bruker AvanceII 300 spectrometer equipped with a QNP probehead. The chemical shifts are given with respect to 85 % H_3PO_4 for ^{31}P (measured by the substitution method) and with respect to tetramethylsilane for ^{1}H (using non deuterated solvent as an internal secondary reference) and ^{13}C (using the solvent peaks as an internal secondary reference). Cyclic voltammetry studies were performed in acetonitrile solution with an EG&G model 273A system using a standard three electrodes cell. The working electrode is a glassy carbon electrode (diameter 3 mm), the reference is a calomel electrode filled with a 3 M LiCl solution (CE) equipped with a double junction, and a platinum wire as the counter electrode. The electrolyte is (n-Bu_4N)BF_4 (0.1 M) and the scan rate is 100 $mV.s^{-1}$ unless otherwise noted. All potentials are given relative to CE. ESI mass spectra were recorded using an ion trap mass spectrometer (Bruker Esquire 3000) equipped with an orthogonal ESI source. Sample solutions (50 µM in acetonitrile) were injected into the ESI source using a syringe pump with a flow rate of 120 $\mu L.min^{-1}$. The capillary high voltage was set to 3500 V. The capillary exit and first skimmer were varied between -18.0 and -45.0 V for the former and -8.0 and -15.0 V for the latter, in order to identify peaks due to in-source decomposition.

Synthesis. $K_7[PW_{11}O_{39}].14H_2O$,[29] ($n$-$Bu_4N$)[$Ru^{VI}NCl_4$],[30] ($n$-$Bu_4N$)$_4$[$PW_{11}O_{39}Ru^{VI}N$] (($n$-$Bu_4N$)$_4$**1**)[20] were prepared following the published procedures; their purity was checked by infrared spectroscopy and, when applicable, by ^{1}H or ^{31}P NMR spectroscopy. Reagent grade solvents and reagents were used as received unless specifically indicated. (n-Bu_4N)OH (initially 40 % by weight in methanol) was titrated by 0.1 M HCl in water before use.

(n-Bu_4N)$_3$[$PW_{11}O_{39}Ru^{V}${$NPPh_3$}] ((n-Bu_4N)$_3$2) Compound **2** was prepared by a modification of the previously published procedure.[20] To a green solution of (n-Bu_4N)$_4$[$PW_{11}O_{39}Ru^{VI}N$] ((n-Bu_4N)$_4$**1**) (665 mg in 15 mL CH_3CN, 0.18 mmol) was slowly added a 1:1 mixture of PPh_3 (48 mg, 0.18 mmol) and *para*-toluenesulfonic acid monohydrate (33 mg, 0.18 mmol) dissolved in 5 mL of CH_3CN. The resulting orange solution was poured into 200 mL of diethylether under agitation, yielding an orange precipitate. Purification was achieved by column chromatography using a 10 cm wide column, 850 mL of wet silica gel 60 (0.063-0.200 nm particle size) and 1:1 mixture of acetonitrile and methylene chloride as eluent. The first orange fraction was evaporated to dryness by rotary evaporation at 35°C, yielding 580 mg (84 %) of (n-Bu_4N)$_3$**2** as a red-orange powder. IR (KBr) ν_{max} (cm^{-1}): 388 (s), 518 (m), 690 (w), 724 (w), 806 (vs), 886 (s), 969 (s), 1049 (m), 1087 (s), 1114 (w), 1381 (w), 1438 (w), 1484 (m), 2874 (w), 2833 (w), 2962 (m). Raman ν_{max}

(cm^{-1}): 165 (m), 213 (m), 227 (w), 252 (w), 528 (m), 661 (m), 900 (m), 988 (vs), 1027 (w), 1103 (w), 1318 (w), 1449 (w), 1588 (w), 2892 (w). UV (CH_3CN) λ_{max} (nm) (log ε): 442 (3.7). ^{31}P NMR (121.5 MHz, CD_3CN, 300 K) δ (ppm): 322 ($\Delta\nu_{1/2}$ = 90 Hz). ^{1}H NMR (300.13 MHz, CD_3CN, 300 K) δ (ppm): 1.00 (t, 36H, ($CH_3(CH_2)_3)_4N^+$), 1.41 (h, 24H, ($CH_3CH_2(CH_2)_2)_4N^+$), 1.67 (m, 24H, ($CH_3CH_2CH_2CH_2)_4N^+$), 3.16 (m, 24H, ($CH_3(CH_2)_2CH_2)_4N^+$), 7.57 (t, J = 7.0 Hz, 3H, p-C_6H_5), 9.44 (d, J = 5.6 Hz, 6H, m-C_6H_5), 12.05 (br, $\Delta\nu_{1/2}$ = 25 Hz, 6H, o-C_6H_5). ^{13}C NMR (75.6 MHz, CD_3CN, 300 K) δ (ppm): 14.1, 20.7, 24.7, 59.7, 143.9, 147.9, 190.3. ESI-MS: m/z (Da) 931 ([**2** - PPh_3]$^{3-}$, degradation *in situ*), 1018 ([**2**]$^{3-}$), 1528 ([H**2**]$^{2-}$), 1649 ([(n-Bu_4N)**2**]$^{2-}$). CV $E_{1/2}$ (mV *vs.* CE in CH_3CN) ($\Delta E_{1/2}$, mV) -713 (122), 311 (73). EPR[20] g_1=2.51, g_2=2.32, g_3=1.68.

(n-Bu_4N)$_4$[$PW_{11}O_{39}Ru^{III}${N(OH)PPh_3}] ((n-Bu_4N)$_4$3) Compound **3** can be prepared by careful addition of (n-Bu_4N)OH to a solution of (n-Bu_4N)$_3$[$PW_{11}O_{39}Ru^{V}${NPPh_3}] ((n-Bu_4N)$_3$**2**) monitored by ^{31}P NMR and UV-visible spectroscopy. The synthesis from (n-Bu_4N)$_4$[$PW_{11}O_{39}Ru^{VI}$N] ((n-Bu_4N)$_4$**1**) described below, however, allows skipping the lengthy chromatography step involved in the preparation of **2**. Also, the smaller amount of (n-Bu_4N)OH added makes the solution of **3** more stable. A green solution of **1** was prepared by dissolution of 250 mg (66 µmol) of (n-Bu_4N)$_4$[$PW_{11}O_{39}Ru^{VI}$N] ((n-Bu_4N)$_4$**1**) in 10 mL of CH_3CN freshly distilled over CaH_2 and cooled down to 0°C in an ice bath. To this vigorously stirred solution was added *via* a dropping funnel (1 drop every 10 s) 5 mL of a solution of PPh_3 (13.3 mM, 66 µmol) and (n-Bu_4N)OH (7.32 mM, 37 µmol) prepared from PPh_3, (n-Bu_4N)OH stock solution and freshly distilled acetonitrile. If the presence of (n-Bu_4N)$_3$[$PW_{11}O_{39}Ru^{V}${NPPh_3}] is detected by ^{31}P NMR, an extra amount of (n-Bu_4N)OH can be carefully added, until only the desired product is present. This solution of **3** (4.4 mM, no impurity detected by ^{31}P NMR) can be stored for months at liquid nitrogen temperature but decomposes in a few hours at room temperature. Raman (4.4 mM in acetonitrile) ν_{max} (cm^{-1}): 600 (br, m), 799 (m), 830 (w), 877 (w), 978 (m), 996 (w), 1036 (w), 2116 (m). UV (CH_3CN) λ_{max} (nm) (log ε): 405 (4.1). ^{31}P NMR (121.5 MHz, CD_3CN, 300 K) δ (ppm): 449 ($\Delta\nu_{1/2}$ = 90 Hz). ^{1}H NMR (300.13 MHz, CD_3CN, 300 K) δ (ppm): 9.82, ($\Delta\nu_{1/2}$ = 17 Hz), 19.2 ($\Delta\nu_{1/2}$ = 15 Hz). MS : m/z (Da) 947 ([H**3** - PPh_3]$^{3-}$, degradation *in situ*), 1024 ([H**3**]$^{3-}$), 1105 ([(n-Bu_4N)**3**]$^{3-}$), 1778 ([(n-Bu_4N)$_2$**3**]$^{2-}$).

(n-Bu_4N)$_4$[$PW_{11}O_{39}Ru^{III}${OPPh_3}] ((n-Bu_4N)$_4$4) Compound **4** forms quantitatively when a solution of **3** (see above) is allowed to sit at room temperature. However, completion of the reaction, as determined by ^{31}P NMR, is achieved after one or two days only. Alternatively, a solution of **4** can be prepared more rapidly from the solution of **3** obtained above by addition of (n-

Bu_4N)OH: 15 mL of the 4.4 mM solution of **3** (66 µmol) were brought back to room temperature and 0.52 mL of a 127 mM (*n*-Bu_4N)OH solution prepared by dilution in acetonitrile of the commercial stock solution (66 µmol, one equivalent), were then added in 0.05 mL portions. The solution turned from deep orange to dark brown. Addition of 30 mL of diethylether induced the precipitation of 200 mg of (*n*-Bu_4N)$_4$**4** (75 % yield based on initial (*n*-Bu_4N)$_4$[$PW_{11}O_{39}Ru^{VI}N$]). Brown cubic crystals of (*n*-Bu_4N)$_4$**4** (160 mg, 60 % yield based on initial (*n*-Bu_4N)$_4$[$PW_{11}O_{39}Ru^{VI}N$]) were grown in two days from an acetonitrile solution under diethyl ether diffusion. IR (KBr) ν_{max} (cm^{-1}): 377 (s), 495 (m), 516 (m), 588(s), 693 (w), 721 (w), 784(vs), 801(vs), 877 (s), 957 (s), 1002 (w), 1041 (m), 1078 (s), 1112 (w), 1152 (w), 1381 (w), 1438 (w), 1484 (m), 2874 (w), 2935 (w), 2962 (m). Raman ν_{max} (cm^{-1}): 212 (m), 236 (m), 335 (w), 380 (m), 468 (m), 498 (m), 687 (w), 797 (s), 872 (s), 961 (vs), 975 (vs), 1000 (m), 1029 (m), 1040 (m), 1105 (m), 1318 (w), 1460 (w), 1590 (w), 2892 (m). UV (CH_3CN): λ_{max} (nm) (log ε): 360 (3.9) ^{31}P NMR (121.5 MHz, CD_3CN, 300 K) δ (ppm): -400 ($\Delta\nu_{1/2}$ = 875 Hz), 190 ($\Delta\nu_{1/2}$ = 270 Hz). ^{1}H NMR (300.13 MHz, CD_3CN, 300 K) δ (ppm): 1.02 (t, 48H, ($CH_3(CH_2)_3)_4N^+$), 1.44 (h, 32H, ($CH_3CH_2(CH_2)_2)_4N^+$), 1.68 (m, 32H, ($CH_3CH_2CH_2CH_2)_4N^+$), 3.19 (m, 32H, ($CH_3(CH_2)_2CH_2)_4N^+$), 7.55 (t, J = 5.9 Hz, 3H, *p*-C_6H_5), 7,73 (br, $\Delta\nu_{1/2}$ = 50 Hz, 6H, *o*-C_6H_5, 8.90 (d, J = 5.7 Hz, 6H, *m*-C_6H_5)). ESI-MS: *m/z* (Da) 932 ([H**4** - PPh_3]$^{3-}$, degradation *in situ*), 1019 ([H**4**]$^{3-}$), 1650 ([H(*n*-Bu_4N)**4**]$^{2-}$), 1771 ([(*n*-$Bu_4N)_2$**4**]$^{2-}$). Crystallographic data: cubic, space group: *I*43*m*, *a*=17.59 Å, *V*=5440 Å^3.

(*n*-$Bu_4N)_4[PW_{11}O_{39}Ru^{III}(OH_2)]$ ((*n*-$Bu_4N)_4$5) This compound was prepared using Rong and Pope's synthesis,[24] except that $[Ru^{II}(DMF)_6](OSO_3CF_3)_2$[31] (DMF = *N,N*-dimethylformamide) was used instead of $[Ru^{II}(OH_2)_6](OSO_3CF_3)_2$ for preparation of the intermediate $Cs_4[PW_{11}O_{39}Ru^{III}\{OH_2\}]$. IR (KBr) ν_{max} (cm^{-1}): 374 (m), 390 (m), 513 (w), 800 (vs), 883 (s), 961 (s), 1047 (m), 1082 (s), 1381 (m), 1484 (s), 2876 (s), 2937 (m), 2963 (s). Raman ν_{max} (cm^{-1}): 212 (m), 225 (m), 310 (w), 323 (m), 800 (m), 878 (m), 970 (sh), 979 (s), 1043 (w), 1130 (w), 1460 (w), 2285 (w), 2892 (m). UV (CH_3CN) λ_{max} (nm) (log ε) 360 (3.3). ^{31}P NMR (121.5 MHz, CD_3CN, 300 K) δ (ppm): -70 ppm ($\Delta\nu_{1/2}$ = 1000 Hz).[24] CV $E_{1/2}$ (mV *vs*. SCE in CH_3CN) ($\Delta E_{1/2}$, mV): -1600 (100), -240 (80), 950 (300).

Reaction of (*n*-$Bu_4N)_3[PW_{11}O_{39}Ru^{V}\{NPPh_3\}]$ with PPh_3 To an orange solution of (*n*-$Bu_4N)_3[PW_{11}O_{39}Ru^{V}\{NPPh_3\}]$ (28.3 mg in 2 mL CH_3CN, 7.5 µmol) were successively added 1 mL of a 29 mM solution of *para*-toluenesulfonic acid (29 µmol) and 1 mL of a 7.5 mM solution of PPh_3 (7.5 µmol). The solution slowly turned brown. The sole products detected by ^{31}P NMR after

three days of reaction were $[Ph_3PNPPh_3]^+$ (δ = 22 ppm) and $[PW_{11}O_{39}Ru^{III}(OH_2)]^{4-}$ (**5**) (δ = -70 ppm).

X-Ray absorption spectroscopies. XANES and EXAFS data were obtained at the Soleil synchrotron source, on the SAMBA beamline. The spectra were recorded at the ruthenium K edge (22 117 eV). Detection in transmission mode at liquid nitrogen temperature was used for solid samples ground and pressed into a pellet. Spectra of $(n\text{-}Bu_4N)_4[PW_{11}O_{39}Ru^{III}\{N(OH)PPh_3\}]$ ($(n\text{-}Bu_4N)_4$**3**) as a frozen acetonitrile solution (4.4 mM, *i. e.* about 400 ppm weight in ruthenium) were recorded at liquid nitrogen temperature with fluorescence detection. The experiments were calibrated with a foil of metallic ruthenium. After background correction, the XANES spectra were normalized at 22 230 eV. The EXAFS analysis was performed using the "EXAFS pour le MAC" package.[32] The EXAFS signal was extracted from the raw data by subtracting a linear pre-edge background and normalized by the Lengeler-Eisenberger procedure.[33] The pseudo-radial distribution was given by the Fourier transform of $\omega(k)k^3\chi(k)$, where $\chi(k)$ is a Kaiser-Bessel window with a smoothness parameter equal to 3. The *k* limits are 2.8 and 12.1 $Å^{-1}$. Single scattering fit of experimental curves were performed with the RoundMidnight program[34] with *ab initio* amplitude and phase functions calculated in $(n\text{-}Bu_4N)_3[PW_{11}O_{39}Ru^{V}\{NPPh_3\}]$ ($(n\text{-}Bu_4N)_3$**2**), using the FEFF7 code.[35] The FEFF7 code was also used to calculate the theoretical absorption spectrum for $(n\text{-}Bu_4N)_3[PW_{11}O_{39}Ru^{V}\{NPPh_3\}]$ ($(n\text{-}Bu_4N)_3$**2**) using the structure determined by X-Ray diffraction. A marginal improvement of the fit between the calculated and experimental spectra was observed when double scattering was used instead of simple scattering. Longer scattering paths did not improve the results.

Results

Interest in metal-nitrido and metal-imido complexes stems from their general relevance to dinitrogen activation on one hand,[36] and their potential role in carbon-nitrogen bond formation on the other.[4,5,37-41] Ruthenium nitrido complexes have been far less studied than their osmium analogues,[22,42,43] although the reactivity of the {RuN} function appears to be more dependent upon the ancillary ligands.[43,44] However, this function is generally expected to be electrophilic,[45] as we have indeed verified. Following the report of our preliminary results,[20] we present here a more comprehensive study of the reactivity of complexes $(n\text{-}Bu_4N)_4[PW_{11}O_{39}Ru^{VI}N]$ ($(n\text{-}Bu_4N)_4$**1**) and $(n\text{-}Bu_4N)_3[PW_{11}O_{39}Ru^{V}\{NPPh_3\}]$ ($(n\text{-}Bu_4N)_3$**2**).

Reaction of $[PW_{11}O_{39}Ru^{VI}N]^{4-}$ with PPh_3. The reaction of **1** with one equivalent of triphenylphosphine in acetonitrile, monitored by ^{31}P NMR, yields a mixture of two species: **2** and **3**.

The isolation and characterization of the former has been described in a previous paper.[20] We noticed that the yield of **2** after separation by chromatography on a silica column (70%) was higher

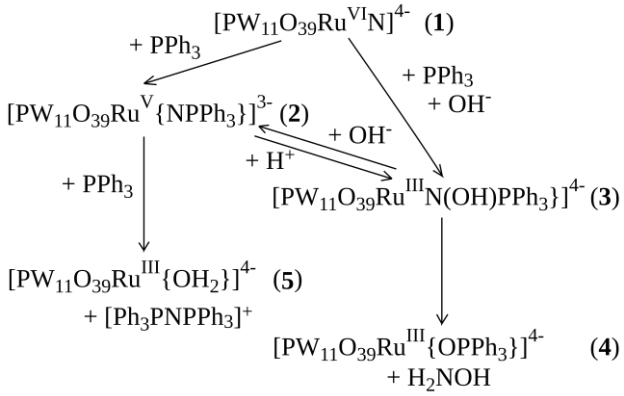

Scheme 1:

than an expected, while any trace of **3** disappeared. This prompted us to investigate the acid-base reactivity of those species. Indeed, **3** is cleanly converted to **2** by addition of one equivalent of a strong acid, thereby explaining our previous observation. Retro-conversion of **2** to **3** can be achieved by the addition of one equivalent of (*n*-Bu_4N)OH or any stronger base (Scheme 1), which led us to formulate **3** as (*n*-$Bu_4N)_4[PW_{11}O_{39}Ru^{III}\{N(OH)PPh_3\}]$ (for assignment of the Ru-oxidation state see below). It should be noted however that at variance with what is usually observed in aqueous solution, the acid-base reactions reported here involve exchange of a hydroxide anion rather than a proton. Regardless of whether a strong base or a sufficient excess of a weaker base such as NEt_3 is used, water inevitably present in the acetonitrile solution quickly yields OH^- as the reacting species. The concentration of water in acetonitrile can easily reach millimolar concentrations,[46,47] and even shortly after distillation, there is a hundredfold excess of water over **2** at the low concentration used for UV-visible spectra. The reaction between **2** and OH^-, monitored by stopped-flow in the UV-visible range is first order with respect to each reagent, with a rate constant of 2.10^6 $M^{-1}.s^{-1}$ at 21°C. This extremely fast reaction suggests a minimal rearrangement between **2** and **3**. Under the same conditions, the reaction between **3** and *para*-toluenesulfonic acid is completed in less than 2 ms. We could also achieve the selective and direct preparation of either **2** or **3** from **1** by adding PPh_3 in the presence of protons or hydroxides respectively, under ^{31}P monitoring.

Further reaction of $[PW_{11}O_{39}Ru^{V}\{NPPh_3\}]^{3-}$ with a second equivalent of PPh_3 in an acidic acetonitrile solution yields the bis(triphenylphosphane)iminium cation $[Ph_3PNPPh_3]^+$ and $[PW_{11}O_{39}Ru^{III}(OH_2)]^{4-}$ (**5**) as sole products identified by their ^{31}P NMR chemical shifts compared to those of authentic samples, thus achieving in two steps complete nitrogen atom transfer from the nitrido polyoxometalate, **1**, to PPh_3. A similar reaction involving $[Os^{IV}(tpy)Cl_2(NPPh_3)]^+$ (tpy = terpyridine) has been reported[22] but an excess of PPh_3 had to be used in that case.

While **2** is stable in solution and in the solid state, its hydroxo derivative, **3**, is hydrolyzed in solution in a matter of minutes to hours, depending on the temperature, the concentration and the

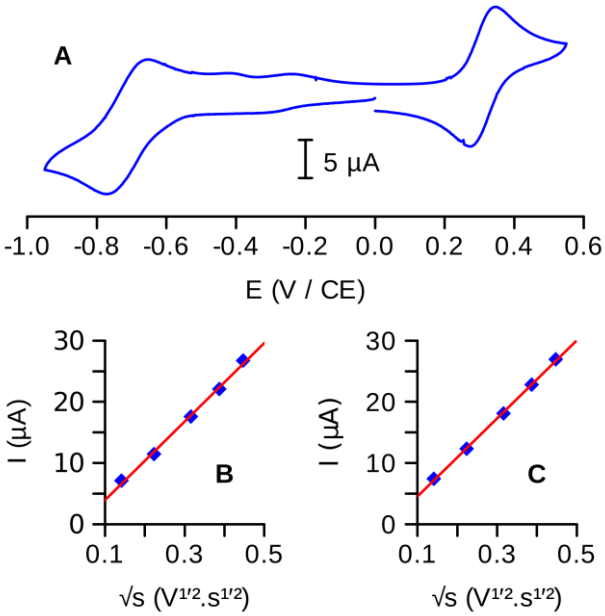

Figure 1A: Cyclic voltammetry of $(n\text{-Bu}_4\text{N})_3[PW_{11}O_{39}Ru^{V}\{NPPh_3\}]$ ($(n\text{-Bu}_4\text{N})_3$**2**) in CH_3CN at a glassy carbon electrode (rate 100 $mV.s^{-1}$, calomel reference electrode). **B**: Plot of $\Delta I = i_{ox}\text{-}i_{red}$ as a function of the square root of the scanning speed for the Ru^{V}/Ru^{IV} couple. **C**: Plot of $\Delta I = i_{ox}\text{-}i_{red}$ as a function of the square root of the scanning speed for the Ru^{VI}/Ru^{V} couple.

basicity of the solution. This hydrolysis selectively produces a single polyoxometalate **4** characterized by two broad signals in ^{31}P NMR. Alternatively, **4** can be prepared more rapidly by addition of $(n\text{-Bu}_4\text{N})OH$ to a solution of **3**, under ^{31}P monitoring. We assign this product as $(n\text{-Bu}_4\text{N})_4[PW_{11}O_{39}Ru^{III}\{OPPh_3\}]$ ($(n\text{-Bu}_4\text{N})_4$**4**), with hydroxylamine as the likely by-product (*cf.* Scheme 1). Furthermore, every attempt to precipitate **3** leads to mixtures of **2** and **4** with no or very little **3** present. All studies on **3** were consequently completed in solution.

Oxidation states. The now well-established ability of lacunary polyoxometalates to stabilize both high and low oxidation state transition metals was illustrated for ruthenium more than fifteen years ago when Rong and Pope isolated and characterized derivatives of the monolacunary polyoxotungstate $[PW_{11}O_{39}]^{7-}$ with the ruthenium center ranging from Ru(II) to Ru(IV). The oxoruthenium (V) species, though not isolated, was also implicated as an intermediate in oxidation reactions.[24] But the drawback of this versatility of polyoxometalates as ligands is that changes of oxidation state sometimes happen unexpectedly.[48] According to the literature, one would expect the product of the reaction between $[PW_{11}O_{39}Ru^{VI}N]^{4-}$ and PPh_3 to be a ruthenium (IV) species.[23,49] But even if phosphorus is indeed oxidized from +III to +V, the oxidation state of ruthenium is decreased by only one unit to yield $[PW_{11}O_{39}Ru^{V}\{NPPh_3\}]^{3-}$ as the only product.[20] The cyclic voltammogram of **2** displays at 0.31 and - 0.71 V/CE two quasi-reversible waves (see Figure 1) that

we suggest to attribute respectively to the Ru^{VI}/Ru^{V} and the Ru^{V}/Ru^{IV} couples, since both oxidation states VI and IV are precedented in ruthenium susbtituted POMs. Additional waves below -1.20 V/CE mark the first reductions of the tungsten framework, with a possible contribution from a

Species	**1**	**2**	**3**	**4**	**5**[a]	$[Ph_3PNPPh_3]^{+}$ [a]
δ_{exp} (ppm)	-13.8	322	449	-400, 190	-70	22
$\Delta\nu_{1/2}$ (Hz)	1	90	90	875, 270	1000	0.7

a: Compared to an authentic sample

Table 1: ^{31}P NMR chemical shifts and half-widths (CD_3CN, 300 K)

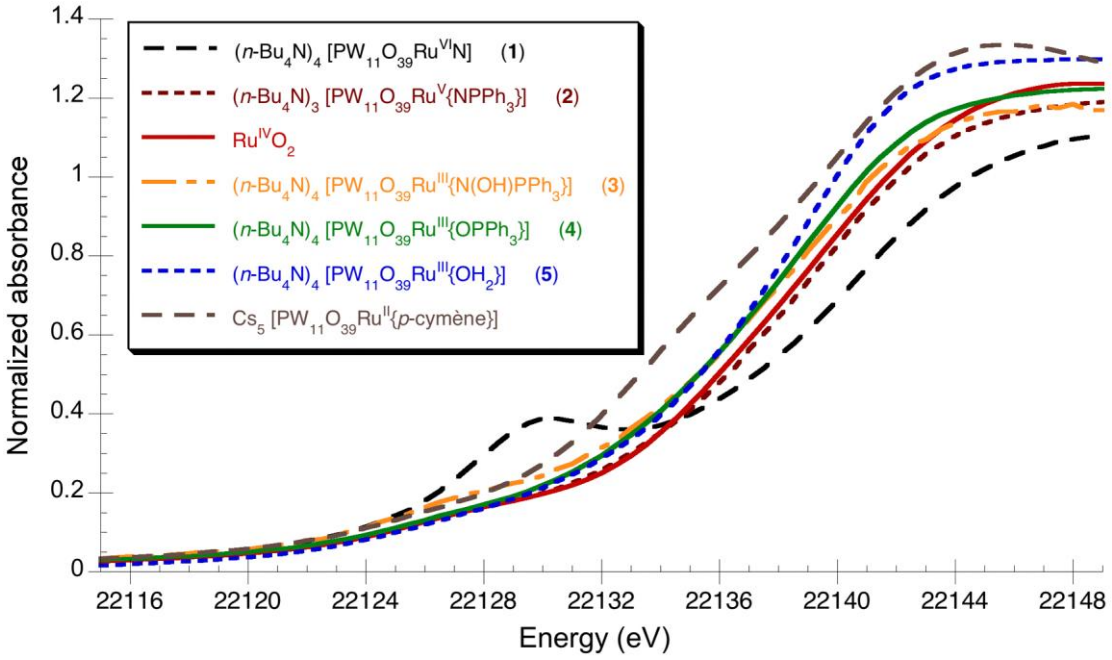

Figure 2: Ru-K edge XANES spectra

Ru^{IV}/Ru^{III} couple. The values for the Ru^{VI}/Ru^{V} and Ru^{V}/Ru^{IV} couples are remarkably low, testifying of the excellent ability of the polyoxometalate framework to stabilize the high oxidation states of the ruthenium atom. A relatively easy oxidation of the putative intermediate $[PW_{11}O_{39}Ru^{IV}\{NPPh_3\}]^{4-}$ is thus expected. The intervention of dioxygen as the potential oxidant, however, can be ruled out, since conducting the reaction under Ar or O_2 results in the same products and kinetics. Consequently, one of our main concerns was to reliably identify the ruthenium oxidation state in the different species we present here.

Our primary tool for assessing the speciation of polyoxometalates is ^{31}P NMR, but this technique provides little further information on the oxidation state. Still, the position and width of the peaks (Table 1) are indicative of the magnetic properties of the ruthenium center: diamagnetic (Ru^{VI} in **1**, Ru^{II}) or paramagnetic (Ru^{V} in **2**, Ru^{III} in **3**, **4** and **5**). Further, the NMR data might not

always be conclusive since a ruthenium (IV) center might be either dia- or paramagnetic.[5,23,50-52] X-ray absorption near edge spectroscopy (XANES) at the ruthenium K edge is the technique of choice to determine the oxidation state of the metal center. Figure 2 shows the spectra for reference

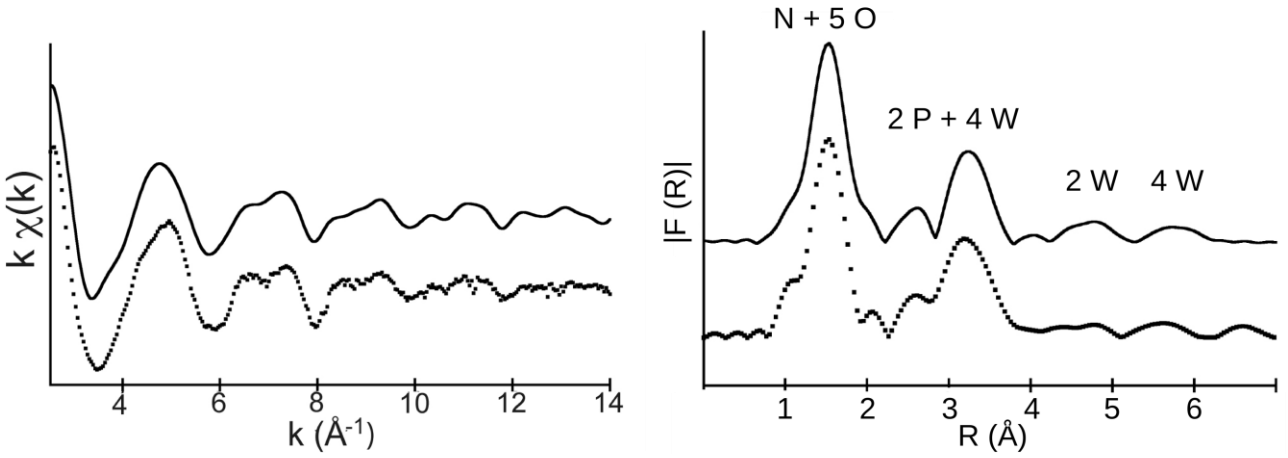

Figure 3: Ru-K edge EXAFS signal of (n-Bu_4N)$_3$[$PW_{11}O_{39}Ru^{V}${NPPh$_3$}] (n-Bu_4N)$_3$**2**) and its Fourier transform: calculated (plain line) and experimental (dotted).

compounds $Cs_5[PW_{11}O_{39}Ru^{II}\{p\text{-cymene}\}]$, ($n$-$Bu_4N$)$_4$[$PW_{11}O_{39}Ru^{III}${OH$_2$}] (($n$-$Bu_4N$)$_4$**5**), $Ru^{IV}O_2$ and (n-Bu_4N)$_4$[$PW_{11}O_{39}Ru^{VI}$N] ((n-Bu_4N)$_4$**1**) as well as those of (n-Bu_4N)$_3$**2**, (n-Bu_4N)$_4$**3** and (n-Bu_4N)$_4$**4**. All spectra were recorded in transmission on solid samples except for (n-Bu_4N)$_4$**3**, whose spectrum was registered from a frozen 4.4 mM acetonitrile solution (about 400 ppm of Ru in weight) by detection of fluorescence. Since the environment of the ruthenium, a distorted octahedron constituted mainly of oxygen atoms, is similar in all those species, the position of the edge is expected to be a function of the oxidation state only. The data indicate this is actually the case, with the energy of the edge increasing as the oxidation state of the ruthenium increases. The edge for **2** lies between the edges of the Ru^{IV} and Ru^{VI} references, thereby confirming the oxidation state of the iminophosphorane derivative as +V, in accordance with our previous findings.[20] On the other hand, the edges for **3** and **4** are very close to those of **5** and [Ru^{III}(acac)$_3$] (acac = acetylacetonate, not shown) which indicate that these compounds contain ruthenium +III.

EXAFS. Slow diffusion of ether into an acetonitrile solution of (n-Bu_4N)$_4$**4** yields crystals suitable for X-ray diffraction. Unfortunately, they belong to the cubic crystallographic system with the well-known unit cell characterized by a=17.59 Å and V=5440 Å, often encountered in α-Keggin compounds of global charge -4 and this precludes any detailed analysis by X-ray diffraction. The asymmetric unit indeed displays only one averaged metallic center composed of 11/12 W and 1/12 Ru, one disordered terminal ligand, one doubly bridging oxygen and one quadruply bridging oxygen linked to phosphorus, as previously observed.[48] The disorder observed in the crystal however indirectly indicates that the ruthenium atom lies in an « in-pocket » position,

the polyoxometalate framework providing five coordination sites in a similar fashion to what is observed in **1**, **2** and **5**, and not in the out-of-pocket position in which the bonds between the Ru, the heteroatom oxygen and two oxygens of the lacuna are broken, as it sometimes happens.[53-56]

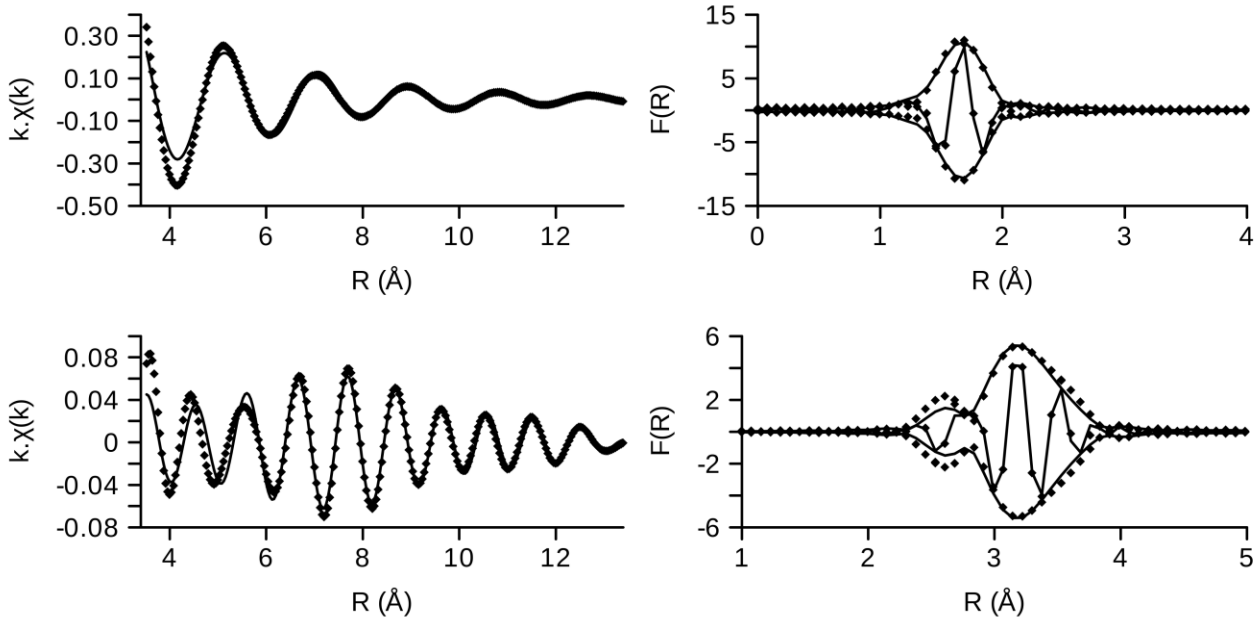

Figure 4: First (above) and second (below) shell filters of the EXAFS spectrum and Fourier transform of (n-$Bu_4N)_4[PW_{11}O_{39}Ru^{III}\{OPPh_3\}]$ ((n-$Bu_4N)_4$**4)**: experimental (dotted line) and simulated (plain).To address such an issue, extended X-ray absorption fine structure

spectroscopy (EXAFS) analysis has been carried out. The iminophosphorane derivative **2**, whose structure we know from the X-ray diffraction, can be used as a benchmark for the EXAFS study of other compounds of similar structure (Figure 3). Optimization of the parameters requested to simulate the spectrum indicates that the environment of the ruthenium center in **2** is constituted by four Ru-O bonds at 1.96(3) Å, one Ru-O bond at 2.15(6.5) Å and one Ru-N bond at 1.87(3) Å, in agreement with the distances of 1.962(13) (average value), 2.200(11) and 1.923(16) Å obtained from the X-ray structure. The second shell is found to be constituted by two tungstens at 3.24(5.2) Å, two tungstens at 3.58(5.3) Å and two phosphorus atoms at 3.19(3.7) and 3.30(3.7) Å, versus 3.302(2) and 3.611(2) Å for the Ru-W and 3.199(11) and 3.307(5) Å for the Ru-P distances in the crystal. Further contributions in the Fourier transform of the EXAFS signal could be attributed to tungsten atoms as far off as 6 Å from the ruthenium center.

The EXAFS and Fourier transform signals of **2** and **4** display only few differences. The first shell of neighbors, albeit similar in overall shape, lies about 0.05 Å further from the ruthenium in **4**, which is consistent with the lower oxidation state of the metal. However, the second shell is almost exactly identical in both cases, validating the hypothesis concerning the presence of the phosphorus-containing ligand as well as the fact that the ruthenium lies completely in the lacuna, the polyoxometalate acting as pentadentate ligand. The environment of the ruthenium, as obtained

from the optimization of the simulation of the EXAFS and Fourier transform signals (Figure 4),

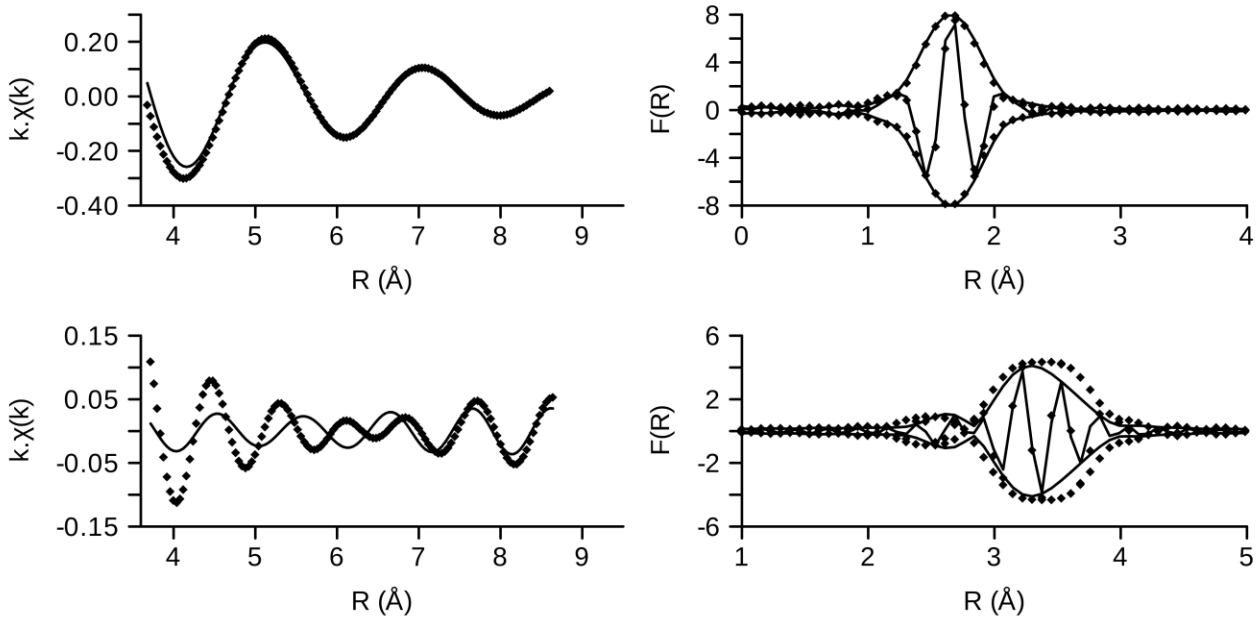

Figure 5: First (above) and second (below) shell filters of the EXAFS spectrum and Fourier transform of $(n\text{-}Bu_4N)_4[PW_{11}O_{39}Ru^{III}\{N(OH)PPh_3\}]$ ($(n\text{-}Bu_4N)_4$**3**): experimental (dotted line) and simulated (plain). The bad agreement at low *k* values for the second shell is due to the very low signal to noise ratio.

consists of a first shell of six oxygens (4×2.01(5.4) Å, 1×2.45(6) Å, 1×1.97(5.4) Å) and a second shell of four tungstens (2×3.24(5.5) Å, 2×3.57(5.5) Å) and two phosphorus atoms (3.32(5.5) Å).

Since **3** cannot be isolated in the solid state, it is impossible to use EXAFS in transmission mode as we did for **2** and **4**. However, thanks to the high intensity of the X-ray beam at the Soleil synchrotron facility, we were able to work in fluorescence mode on a frozen acetonitrile solution. Despite the relatively high level of noise due to low ruthenium concentration (4.4 mM, about 400 ppm), the close similitude between the EXAFS data and Fourier transform signals of **3** and **4** point to a parent structure for both compounds. The optimization of the parameters requested to simulate the spectrum indicates the following distances around the ruthenium center: 2.02(6.5) Å (4xRu-O_W), 2.48(7.2) Å (Ru-O_P), 1.99(6.5) Å (Ru-N), 3.29(5.3) Å (2xRu-W), 3.59(5.2) Å (2xRu-W), 3.20(6.5) Å (Ru-P_{Ph}), 3.36(5.5) Å (Ru-P_O) (Figure 5), emphasizing the kinship between **3** and **4**. We can therefore conclude from the XAS data that in both **3** and **4** the lacunary polyoxometalate $[PW_{11}O_{39}]^{7-}$ acts as a pentadentate ligand towards a ruthenium (III) center and the sixth ligand is a triphenylphosphine derivative.

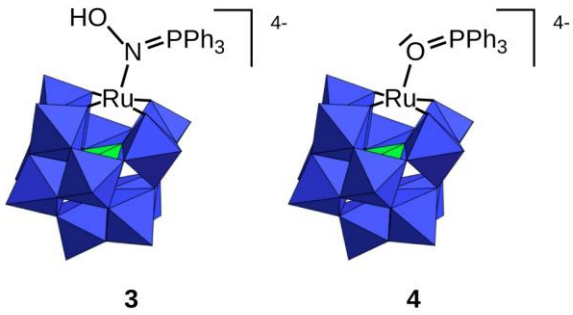

3 4

Figure 6: Proposed structures of $[PW_{11}O_{39}Ru^{III}\{N(OH)PPh_3\}]^{4-}$ (**3**) (left) and $[PW_{11}O_{39}Ru^{III}\{OPPh_3\}]^{4-}$ (**4**) (right).

Discussion

Structure of compound 4. Several lines of evidence led us to formulate compound **4** as $[PW_{11}O_{39}Ru^{III}\{OPPh_3\}]^{4-}$ and to propose the structure shown in Figure 6. The incorporation of one ruthenium atom in the $[PW_{11}O_{39}]^{7-}$ framework is indicated at first by the dark brown color of the solution, caused by a broad charge transfer band (λ_{max} = 360 nm , log(ε) = 3.9) and was confirmed by mass spectrometry as well as by the intensity of the X-ray absorption during the XAS experiments. The complete incorporation of the ruthenium in the lacuna ("in-pocket" configuration) is supported by the EXAFS data and by crystallization in a cubic space group.

The oxidation state of the ruthenium was found to be +III by XANES (see previous paragraph), with an edge close to what is observed for $[PW_{11}O_{39}Ru^{III}\{OH_2\}]^{4-}$ (**5**). The similarity between the electronic properties of those two compounds is also indicated by the identical positions (albeit with different absorption coefficients) of their charge transfer band. This in turn indicates that the overall charge of those two species is likely to be the same, *i. e.* that the ruthenium in **4** bears a neutral ligand.

The incorporation of a ligand derived from PPh_3 in **4** is suggested by the observation of two signals in its ^{31}P NMR spectrum (Table 1) and is confirmed by mass spectrometry and ^{1}H NMR, IR and Raman spectroscopies. The presence in the IR spectrum of a band at 1112 cm^{-1} is very close to the PN double bond stretching mode in **2** (1114 cm^{-1}) which suggests the presence of a P=X bond, where X is either oxygen or nitrogen (discrimination between these two is impossible from mass spectrometry because of the broadness of the peaks generated by the wide isotopic distribution of tungsten). We infer from the electrochemical study that the reduction of the iminophosphorane derivative of ruthenium +IV is very probably centered on the tungsten framework, which rules out a reduced form of **2**. The structure of **4** is thus likely $[PW_{11}O_{39}Ru^{III}\{OPPh_3\}]^{4-}$, with the 1112 cm^{-1} IR band assigned to the P=O double bond stretch of the coordinated triphenylphosphine oxide

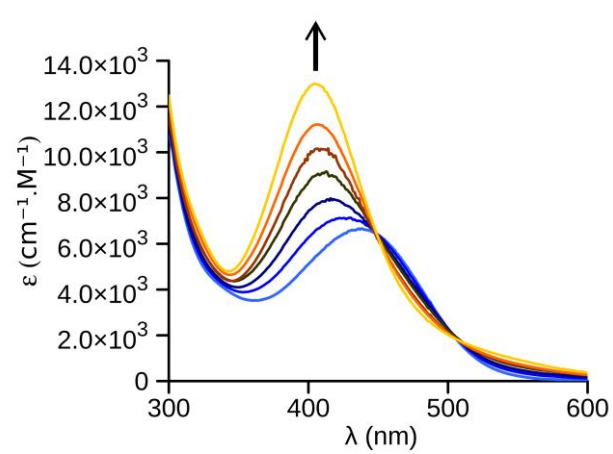

Figure 7: Titration of $[PW_{11}O_{39}Ru^{V}\{NPPh_3\}]^{3-}$ (**2**) by OH^-, yielding $[PW_{11}O_{39}Ru^{III}\{N(OH)PPh_3\}]^{4-}$ (**3**)

molecule. This value is among the lowest reported for PO stretches in transition metal complexes of triphenylphosphine oxide: the free ligand displays this band at 1195 cm^{-1}, while the reported values for coordinated molecules are found between 1105[57] and 1192 cm^{-1}.[58] This relative weakness of the phosphorus-oxygen bond suggests in turn a strong binding of the ligand to the ruthenium center. As a result, we expect the ruthenium to oxygen distance to be rather short when compared with the metal-oxygen distance in other triphenylphosphine oxide complexes, which lie between 1.9[59] and 2.5 Å.[60] Concerning ruthenium, an extended search of the literature yields only a few reports of triphenylphosphine oxide complexes that are fully characterized structurally. Among those, most deal with Ru^{II} derivatives, with Ru-O distances ranging from 2.22[61] to 2.29[62] Å. As expected, the Ru^{III}-O distance in **4** deduced by EXAFS, 1.97 Å, is significantly shorter. The shortness of the bond between the ruthenium and $OPPh_3$, and hence its strength, might be significant in accounting for the stability of compound **4**.

Structure of compound 3. Because of the instability of **3** in solution and the impossibility to isolate it in the solid state, elucidation of its structure was more difficult. The reaction between **2** and **3** implicates a hydroxide exchange (see above). The resulting formulation of **3** as $[PW_{11}O_{39}Ru^{III}\{N(OH)(PPh_3)\}]^{4-}$ is also in agreement with mass spectrometry, Raman and ^1H NMR spectroscopy data, while XANES and EXAFS data underline the structural similarity between **3** and **4**. Next comes the question of the position of the hydroxide fragment. The two most likely possibilities are coordination to the Ru^{V} center or to the nitrogen atom as illustrated in Figure 6. In the first case, the Ru^{V} center would either become seven coordinated or adopt an « out-of-pocket » configuration, thus having coordination sites available for the hydroxide. This possibility is supported by the similarities between the UV-visible spectra of **2** and **3**, with charge transfer bands at 442 nm and 405 nm respectively (Figure 7). However, the out-of-pocket configuration can be ruled out from the EXAFS data which strongly indicate the presence of the "in-pocket"

configuration. The second case is akin to a reductive elimination at the ruthenium center, yielding the neutral triphenylphosphine oxime Ph_3PNOH, coordinated through a dative N-Ru bond to the +III metallic center. This second scenario, with a nucleophilic attack on the nitrogen is consistent with formation of $[Ph_3PNPPh_3]^+$ from **2** and is in accordance with both the XANES and EXAFS data. The reduction of ruthenium from Ru(V) in **2** to Ru(III) in **3** corresponds to an internal electron transfer within the metal-ligand function, akin to the reduction of Ru(VI) by PPh_3 addition to the starting nitrido complex **1**.

Compound **3** is to our knowledge the first phosphine oxime derivative reported, but it can be related to several parent phosphine imine derivatives such as the *N*-methoxytriphenylphosphinimium cation[63] or triphenylphosphinaminoimine.[64,65] Classical imines derivatives are easily hydrolysed to the corresponding ketone, thus it is not surprising that all the aforementioned species tend to decompose quickly in the presence of water to give triphenylphosphine oxide, a fate from which **3** does not escape. Nevertheless, if care is taken to keep a solution of **3** as devoid of extra hydroxide or water molecules as possible, it can be preserved at room temperature for several minutes. In the absence of better structural data, one can only speculate on the origin of this relative stability. The combination of steric and electrostatic repulsion due to the polyoxometalate framework is likely to slow down the reaction between **3** and H_2O or OH^-, but some more subtle electronic effect might also be playing a role.

Summary and conclusion

This study of the reactivity between triphenylphosphine and a ruthenium(VI) nitrido function, embedded in the lacunary polyoxometalate $[PW_{11}O_{39}]^{7-}$, shows that the reaction proceeds in two well-separated steps. The iminophosphorane derivative $[PW_{11}O_{39}Ru^{V}\{NPPh_3\}]^{3-}$ (**2**) we reported earlier[20] is the product of the first, fast step. In the presence of hydroxide, the unstable phosphine oxime complex $[PW_{11}O_{39}Ru^{III}\{N(OH)PPh_3\}]^{4-}$ (**3**) can also form, emphasizing the necessity of a careful control of the acid-base conditions even if only a small amount of water is present, which is almost unavoidable in acetonitrile. Compound **3** will then cleanly convert to $[PW_{11}O_{39}Ru^{III}\{OPPh_3\}]^{4-}$ (**4**). Compound **2** reacts with a second equivalent of triphenylphosphine in a subsequent, slower step, to yield the bis(triphenylphosphane)iminium cation $[Ph_3PNPPh_3]^+$ and $[PW_{11}O_{39}Ru^{III}(OH_2)]^{4-}$, thus achieving complete transfer of the nitrogen atom from the polyoxometalate to the organic substrate. We thus provide some unprecedented insights into the reactivity of a ruthenium iminophosphorane function, in the peculiar environment of the POM.

In the course of this investigation, we characterized two new ruthenium derivatives,

$[PW_{11}O_{39}Ru^{III}\{N(OH)PPh_3\}]^{4-}$ (**3**) and $[PW_{11}O_{39}Ru^{III}\{OPPh_3\}]^{4-}$ (**4**). With the structural characterization of those two compounds by X-ray diffraction being impossible, we had to resort to several other techniques including XANES and EXAFS, mass spectrometry, ^{1}H and ^{31}P NMR, UV-visible, IR and Raman spectroscopies to identify them. Ultimate identification was only possible with the help of thoroughly characterized references such as $[PW_{11}O_{39}Ru^{VI}N]^{4-}$ (**1**), $[PW_{11}O_{39}Ru^{V}\{NPPh_3\}]^{3-}$ (**2**) and $[PW_{11}O_{39}Ru^{III}\{OH_2\}]^{4-}$ (**5**). In the course of this work, we have accumulated spectroscopic data on all those species. Together with Rong and Pope's study[24] as well as others from our laboratory,[20] [15] this study makes the $[PW_{11}O_{39}RuL]^{n-}$ system the most extensively investigated of all ruthenium-substituted polyoxotungstates, with oxidation states of the ruthenium center ranging from +II to +VI, both in water and in acetonitrile. As such, it might prove to be a useful reference for further studies of ruthenium containing polyoxometalates, a subject that is likely to attract much interest in the near future. [17,18,19,66]

Acknowledgment. The present research is supported by the ANR-06-BLAN-0249-01 grant (grant to A. Proust) and by the US Department of Energy grant DE-FG02-03ER15461 (grant to C. L. Hill).

References:

(1) Naota, T.; Takaya, H.; Murahashi, S.-I. *Chem. Rev.* **1998**, *98*, 2599-2660.

(2) Grubbs, R. H. *Angew. Chem. Int. Ed.* **2006**, *45*, 3760-3765.

(3) Liu, F.; Concepcion, J. J.; Jurss, J. W.; Cardolaccia, T.; Templeton, J. L.; Meyer, T. J. *Inorg. Chem.* **2008**, *47*, 1727-1752.

(4) Leung, S. K.-Y.; Huang, J.-S.; Liang, J.-L.; Che, C.-M.; Zhou, Z.-Y. *Angew. Chem. Int. Ed.* **2003**, *42*, 340-343.

(5) Man, W.-L.; Lam, W. W. Y.; Yiu, S.-M.; Lau, T.-C.; Peng, S.-M. *J. Am. Chem. Soc.* **2004**, *126*, 15336-15337.

(6) Hill, C. L.; Prosser-McCartha, C. M. *Coord. Chem. Rev.* **1995**, *143*, 407-455.

(7) Neumann, R. *Prog. inorg. Chem.* **1998**, *47*, 317-370.

(8) Mizuno, N.; Yamaguchi, K.; Kamata, K. *Coord. Chem. Rev.* **2005**, *249*, 1944-1956.

(9) Bi, L.-H.; Reike, M.; Kortz, U.; Keita, B.; Nadjo, L.; Clark, R. J. *Inorg. Chem.* **2004**, *43*, 3915-3920.

(10) Anderson, T. M.; Neiwert, W. A.; Kirk, M. L.; Piccoli, P. M. B.; Schultz, A. J.; Koetzle, T. F.; Musaev, D. G.; Morokuma, K.; Cao, R.; Hill, C. L. *Science* **2004**, *306*, 2074-2077.

(11) Anderson, T. M.; Cao, R.; Slonkina, E.; Hedman, B.; Hodgson, K. O.; Hardcastle, K. I.; Neiwert, W. A.; Wu, S. X.; Kirk, M. L.; Knottenbelt, S.; Depperman, E. C.; Keita, B.; Nadjo, L.; Musaev, D. G.; Morokuma, K.; Hill, C. L. *J. Am. Chem. Soc.* **2005**, *127*, 11948-11949.

(12) Cao, R.; Anderson, T. M.; Piccoli, P. M. B.; Schultz, A. J.; Koetzle, T. F.; Geletii, Y. V.; Slonkina, E.; Hedman, B.; Hodgson, K. O.; Hardcastle, K. I.; Fang, X.; Kirk, M. L.; Knottenbelt, S.; Kögerler, P.; Musaev, D. G.; Morokuma, K.; Takahashi, M.; Hill, C. L. *J. Am. Chem. Soc.* **2007**, *129*, 11118-11133.

(13) Khenkin, A. M.; Kumar, D.; Shaik, S.; Neumann, R. *J. Am. Chem. Soc.* **2007**, *129*, 723-723.

(14) Randall, W. J.; Weakley, T. J. R.; Finke, R. G. *Inorg. Chem.* **1993**, *32*, 1068-1071.

(15) Chen, S.-W.; Villanneau, R.; Li, Y.; Chamoreau, L.-M.; Boubekeur, K.; Thouvenot, R.; Gouzerh, P.; Proust, A. *Eur. J. Inorg. Chem.* **2008**, 2137-2142.

(16) Yamaguchi, S.; Uehara, K.; Kamata, K.; Yamaguchi, K.; Mizuno, N. *Chem. Lett.* **2008**, *37*, 328-329.

(17) Geletii, Y. V.; Botar, B.; Kögerler, P.; Hillesheim, D. A.; Musaev, D. G.; Hill, C. L. *Angew. Chem. Int. Ed.* **2008**, *47*, 3896-3899.

(18) Sartorel, A.; Carraro, M.; Scorrano, G.; Zorzi, R. D.; Geremia, S.; McDaniel, N. D.; Bernhard, S.; Bonchio, M. *J. Am. Chem. Soc.* **2008**, *130*, 5006-5007.

(19) Geletii, Y. V.; Huang, Z.; Hou, Y.; Musaev, D. G.; Lian, T.; Hill, C. L. *J. Am. Chem. Soc.* **2009**, *131*, 7522-7523.

(20) Lahootun, V.; Besson, C.; Villanneau, R.; Villain, F.; Chamoreau, L.-M.; Boubekeur, K.; Blanchard, S.; Thouvenot, R.; Proust, A. *J. Am. Chem. Soc.* **2007**, *129*, 7127-7135.

(21) Dehnicke, K.; Krieger, M.; Massa, W. *Coord. Chem. Rev.* **1999**, *182*, 19-65.

(22) Demadis, K. D.; Bakir, M.; Klesczewski, B. G.; Williams, D. S.; White, P. S.; Meyer, T. J. *Inorg. Chim. Acta* **1998**, *270*, 511-526.

(23) Chan, P.-M.; Yu, W.-Y.; Che, C.-M.; Cheung, K.-K. *J. Chem. Soc. Dalton Trans* **1998**, 3183-3190.

(24) Rong, C.; Pope, M. T. *J. Am. Chem. Soc.* **1992**, *114*, 2932-2938.

(25) Sadakane, M.; Higashijima, M. *Dalton Trans.* **2003**, 659-664.

(26) Sadakane, M.; Tsukuma, D.; Dickman, M. H.; Bassil, B. S.; Kortz, U.; Higashijima, M.; Ueda, W. *Dalton Trans.* **2006**, *35*, 4271-4276.

(27) Sadakane, M.; Tsukuma, D.; Dickman, M. H.; Bassil, B. S.; Kortz, U.; Capron, M.; Ueda, X. *Dalton Trans.* **2007**, 2833-2838.

(28) Mendes, P. Gepasi v. 3.0, *Comput. Applic. Biosc.* **1993**, *9*, 563-571.

(29) Contant, R. *Can. J. Chem.* **1987**, *65*, 568-573.

(30) Griffith, W. P.; Pawson, D. *J. Chem. Soc. Dalton Trans* **1973**, *5*, 1315-1320.

(31) Judd, R. J.; Cao, R.; Biner, M.; Armbruster, T.; Bürgi, H.-B.; Merbach, A. E.; Ludi, A. *Inorg. Chem.* **1995**, *34*, 5081-5083.

(32) Michalowitcz, A. EXAFS version 1998 pour Mac OS9, http://www.univ-

paris12.fr/40615508/0/fiche_3000A_pagelibre/

(33) Lengeler, B.; Eisenberg, P. *Phys. Rev. B* **1980**, *21*, 4507.

(34) Michalowitcz, A. RoundMidnight pour Mac OSX, http://www.univ-paris12.fr/40615508/0/fiche_3000A__pagelibre/

(35) Zabinsky, S. I.; Rehr, J. J.; Ankudinov, J. J.; Albers, R. C.; Eller, M. J. *Phys. Rev. B* **1995**, *52*, 2995-3009.

(36) Schrock, R. R. *Acc. Chem. Res.* **2005**, *38*, 955-962.

(37) Groves, J. T.; Takahashi, T. *J. Am. Chem. Soc.* **1983**, *105*, 2073.

(38) DuBois, J.; Tomooka, C. S.; Hong, J.; Carreira, E. M. *Acc. Chem. Res.* **1997**, *30*, 364-.

(39) Ho, C.-M.; Lau, T.-C.; Kwong, H.-L.; Wong, W.-T. *Dalton Trans.* **1999**, 2411-2413.

(40) Nishimura, M.; Minakata, S.; Thongchant, S.; Ryu, I.; Komatsu, M. *Tet. Lett.* **2000**, *41*, 7089-7092.

(41) Au, S.-M.; Huang, J.-S.; Yu, W.-Y.; Fung, W.-H.; Che, C.-M. *J. Am. Chem. Soc.* **1999**, *121*, 9120-9132.

(42) Meyer, T. J.; Huynh, M. H. V. *Inorg. Chem.* **2003**, *42*, 8140-8160.

(43) Crevier, T. J.; Bennett, B. K.; Soper, J. D.; Bowman, J. A.; Dehestani, A.; Hrovat, D. A.; Lovell, S.; Kaminsky, W.; Mayer, J. M. *J. Am. Chem. Soc.* **2001**, *123*, 1059-1071.

(44) Sellmann, D.; Wemple, M. W.; Donaubauer, W.; Heinemann, F. W. *Inorg. Chem.* **1997**, *136*, 1397-1402.

(45) Eikey, R. A.; Abu-Omar, M.-M. *Coord. Chem. Rev.* **2003**, *243*, 83-124.

(46) Martin, M. W. In *Recommended method for purification of solvents and tests for impurities*; Coetzee, J. F., Ed.; Pergamon Press: Oxford, 1982, p 10.

(47) Artero, V., Thèse de l'Université Pierre et Marie Curie, 2000.

(48) Kwen, H.; Tomlinson, S.; Maatta, E. A.; Dablemont, C.; Thouvenot, R.; Proust, A.; Gouzerh, P. *Chem. Commun.* **2002**, 2970-2971.

(49) Yi, X.-Y.; Lam, T. C. H.; Sau, Y.-K.; Zhan, Q.-F.; Williams, I. D.; Leung, W.-H. *Inorg. Chem.* **2007**, *46*, 7193-7198.

(50) Kuan, S. L.; Tay, E. P. L.; Leong, W. K.; Goh, L. Y.; Lin, C. Y.; Gill, P. M. W.; Webster, R. D. *Organometallics* **2006**, 6134-6141.

(51) Groves, J. T.; Ahn, K.-H. *Inorg. Chem.* **1987**, *26*, 3831-3833.

(52) Leung, W.-H.; Hun, T. S. M.; Hou, H.-w.; Wong, K.-Y. *J. Chem. Soc. Dalton Trans.* **1997**, 237-243.

(53) Artero, V.; Laurencin, D.; Villanneau, R.; Thouvenot, R.; Herson, P.; Gouzerh, P.; Proust, A. *Inorganic Chemistry* **2005**, *44*, 2826-2835.

(54) Laurencin, D.; Villanneau, R.; Gerard, H.; Proust, A. *Journal Of Physical Chemistry A*

2006, *110*, 6345-6355.

(55) Bi, L.-H.; Kortz, U.; Keita, B.; Nadjo, L. *Dalton Trans.* **2004**, 3184-3190.

(56) Laurencin, D.; Proust, A.; Gérard, H. *Inorg. Chem.* **2008**, *47*, 7888-7893.

(57) Barral, M. C.; Jiménez-Aparicio, R.; Priego, J. L.; Royer, E. L.; Urbanos, F. A.; Amador, U. *Inorg. Chem.* **1998**, *37*, 1413-1416.

(58) Arnáiz, F. J.; Aguado, R.; Pedrosa, M. R.; De Cian, A.; Fischer, J. *Polyhedron* **2000**, *19*, 2141-2147.

(59) Abdallaoui, H. E. E.; Rubini, P.; Tekely, P.; Bayeut, D.; Lecomte, C. *Polyhedron* **1992**, *11*, 1795-1800.

(60) Cindric, H.; Vrdoljak, V.; Matkovic-Calogovic, D.; Kamenar, D. *Acta Cryst. A* **1996**, *52*, 3016-3018.

(61) Barral, M. C.; Jiménez-Aparicio, R.; Priego, J. L.; Royer, E. C.; Saucedo, M. J.; Urbanos, F. A.; Amador, U. *Polyhedron* **1995**, *14*, 2419-2427.

(62) Li, Y.; Huang, J.-S.; Xu, G.-B.; Zhu, N.; Zhou, Z.-Y.; Che, C.-M.; Wong, K.-Y. *Chem. Eur. J.* **2004**, *10*, 3486-3502.

(63) Rudchenko, V. F.; Ignatov, S. M.; Kostyanovsky, R. G. *J. Chem. Soc., Chem. Commun.*, **1990**, 261-262.

(64) Zimmer, H.; Singh, G. *J. Org. Chem.* **1964**, *29*, 1579-1581.

(65) Walker, C. C.; Schechter, H. *Tet. Lett.* **1965**, *20*, 1447-1452.

(66) Howells, A. R.; Sankarraj, A.; Shannon, C. *J. Am. Chem. Soc.* **2004**, *126*, 12258-12259.

Table of contents synopsis

The nitrido derivative $(n\text{-}Bu_4N)_4[PW_{11}O_{39}Ru^{VI}N]$ transfers its nitrogen atom to triphenylphosphine to give $[Ph_3PNPPh_3]^+$. The reactivity of intermediate $(n\text{-}Bu_4N)_3[PW_{11}O_{39}Ru^{V}\{NPPh_3\}]$ was investigated. By addition of one equivalent of hydroxide, $[PW_{11}O_{39}Ru^{III}\{N(OH)PPh_3\}]^{4-}$ is obtained. The reaction can be reversed by the addition of a proton. The phosphinoxime $[PW_{11}O_{39}Ru^{III}\{N(OH)PPh_3\}]^{4-}$ decomposes to yield quantitatively $(n\text{-}Bu_4N)_4[PW_{11}O_{39}Ru^{III}\{OPPh_3\}]$. All those species have been thoroughly characterized by mass spectrometry, paramagnetic ^{31}P NMR, IR, Raman, UV-visible, XANES and EXAFS spectroscopies.